European Journal of Radiology 173 (2024) 111358

Contents lists available at ScienceDirect

European Journal of Radiology

journal homepage: www.elsevier.com/locate/ejrad

Research article

The T1-dark-rim: A novel imaging sign for detecting smoldering inflammation in multiple sclerosis

Pablo Naval-Baudin [a,b,c,d,*], Albert Pons-Escoda [a,b,c,d], Albert Castillo-Pinar [a], Ignacio Martínez-Zalacaín [a], Pablo Arroyo-Pereiro [d,e,f], Susanie Flores-Casaperalta [a,b,c], Francis Garay-Buitron [a,b,c], Nahum Calvo [a,b,c], Antonio Martinez-Yélamos [d,e,f], Mónica Cos [a,b,c], Sergio Martínez-Yélamos [d,e,f], Carles Majós [a,b,c]

[a] Radiology Department, Hospital Universitari de Bellvitge, L'Hospitalet de Llobregat, Carrer de Feixa Llarga SN, 08907 Barcelona, Spain
[b] Institut de Diagnòstic Per La Imatge (IDI), L'Hospitalet de Llobregat, Centre Bellvige, Carrer de Feixa Llarga SN, 08907 Barcelona, Spain
[c] Diagnostic Imaging and Nuclear Medicine Research Group, Bellvitge Biomedical Research Institute (IDIBELL), L'Hospitalet de Llobregat, 08907 Barcelona, Spain
[d] Departament de Ciències Clíniques, Facultat de Medicina I Ciències de La Salut, Universitat de Barcelona (UB), Carrer de Casanova 143, 08036 Barcelona, Spain
[e] Multiple Sclerosis Unit, Department of Neurology, Hospital Universitari de Bellvitge, L'Hospitalet de Llobregat, Carrer de Feixa Llarga SN, 08907 Barcelona, Spain
[f] Neurological Diseases and Neurogenetic Research Group, Bellvitge Biomedical Research Institute (IDIBELL), L'Hospitalet de Llobregat, 08907 Barcelona, Spain

ARTICLE INFO

Keywords:
Multiple sclerosis
Susceptibility-weighted imaging
T1-weighted imaging
Magnetic resonance imaging
Rim lesion

ABSTRACT

Purpose: Paramagnetic rim lesions (PRLs), usually identified in susceptibility-weighted imaging (SWI), are a promising prognostic biomarker of disability progression in multiple sclerosis (MS). However, SWI is not routinely performed in clinical practice. The objective of this study is to define a novel imaging sign, the T1-dark rim, identifiable in a standard 3DT1 gradient-echo inversion-recovery sequence, such as 3D T1 turbo field echo (3DT1FE) and explore its performance as a SWI surrogate to define PRLs.

Methods: This observational cross-sectional study analyzed MS patients who underwent 3T magnetic resonance imaging (MRI) including 3DT1TFE and SWI. Rim lesions were evaluated in 3DT1TFE, processed SWI, and SWI phase and categorized as true positive, false positive, or false negative based on the value of the T1-dark rim in predicting SWI phase PRLs. Sensitivity and positive predictive values of the T1-dark rim for detecting PRLs were calculated.

Results: Overall, 80 rim lesions were identified in 63 patients (60 in the SWI phase and 78 in 3DT1TFE; 58 true positives, 20 false positives, and two false negatives). The T1-dark rim demonstrated 97% sensitivity and 74% positive predictive value for detecting PRLs. More PRLs were detected in the SWI phase than in processed SWI (60 and 57, respectively).

Conclusion: The T1-dark rim sign is a promising and accessible novel imaging marker to detect PRLs whose high sensitivity may enable earlier detection of chronic active lesions to guide MS treatment escalation. The relevance of T1-dark rim lesions that are negative on SWI opens up a new field for analysis.

1. Introduction

1.1. Background

Multiple sclerosis is a progressive inflammatory, demyelinating, and neurodegenerative autoimmune disease of the central nervous system (CNS), with the formation of focal and diffuse lesions and leading to atrophy and chronic progressive and irreversible disability in the majority of patients [1]. Numerous potent disease-modifying medications have been formulated for the management of relapsing-remitting MS (RRMS) [2].

There is mounting evidence that prompt administration of high-

Abbreviations: MS, Multiple sclerosis; MRI, magnetic resonance imaging; PPV, positive predictive value; NPV, negative predicting value; RRMS, relapsing-remitting MS; SPMS, secondary progressive MS; SWI, susceptibility-weighted imaging; 3DT1TFE, 3D T1 turbo field echo; SWIp, SWI with phase enhancement; PRLs, paramagnetic rim lesions.

* Corresponding autor at: Radiology Department, Hospital Universitari de Bellvitge, L'Hospitalet de Llobregat, Carrer de Feixa Llarga SN, 08907 Barcelona, Spain.
E-mail address: pablo.naval.idi@gencat.cat (P. Naval-Baudin).

https://doi.org/10.1016/j.ejrad.2024.111358
Received 27 December 2023; Received in revised form 24 January 2024; Accepted 3 February 2024
Available online 5 February 2024

efficacy disease modifying treatments may delay permanent disability progression in patients with high inflammatory activity [3,4]. Furthermore, until recently, disease modifying treatments for MS have not been effective in treating progressive MS (PMS) [2]. However, more recently sanctioned therapies have demonstrated efficacy in decelerating the progression of disability in patients with non-active primary and secondary PMS [5,6]. Given the effectiveness of these treatments in managing MS, it is becoming increasingly important to promptly predict disability progression and conversion to progressive disease forms [7].

Smoldering disease is one of the main drivers of disability progression in MS [5,6] and is characterized by "chronic active" or "smoldering" lesions. These chronic active lesions (CALs), are localized regions of encapsulated primarily microglial activation within the CNS, isolated behind a largely intact blood–brain barrier [6]. A relevant feature of these lesions is the presence of iron-rich microglia on the lesion border [8].

High-field MRI has been used to detect paramagnetic rims around CALs on processed susceptibility weighted imaging (SWI) and phase imaging [9–12]. These paramagnetic rim lesions (PRLs), also termed "iron rim" or "phase rim" lesions, are thus considered an MRI representation of smoldering inflammation. PRLs have been associated with higher levels of disability and more destructive pathological features [11,13–15].

While PRLs offer promising insights into MS characteristics, their detection in standard MRI follow-ups for MS is not straightforward [16]. Furthermore, PRL visualization requires SWI in imaging protocols, but this technique is not a standard recommendation in routine MRI follow-ups for MS patients [17,18]. Furthermore, although several automated PRL-detection research tools have been developed [19–21], application in clinical practice is far from standard.

On the other hand, PRLs exhibit characteristic hypointensity on T1-weighted imaging (T1WI) [11,14,22–24]. Indeed, in a recent study using intensity-normalized 3DT1TFE, it was found that PRLs have distinguishing and semi-quantifiable deep hypointensity that is practically non-existent in other white matter lesions [25,26]. Moreover, building on this insight and our clinical experience, we observed that these deeply hypointense voxels were aligned in a peripheral pattern, manifesting as a "T1-dark rim" sign on 3DT1TFE imaging. Based on this observation, we hypothesized that this novel imaging sign could simplify the detection of PRLs without the need for SWI.

1.2. Objectives

The primary goal is to present a novel imaging sign observed in 3D gradient echo inversion-recovery T1WI, the "T1-dark rim." We aim to evaluate the sensitivity and positive predictive value of this imaging sign in detecting PRLs.

2. Materials and methods

2.1. Study approval

This study was approved by our center's Research Ethics Committee. All patients provided informed consent for the use of their medical data. Only de-identified data were used for analysis.

2.2. Study design, Participants, and clinical data collection

We designed a retrospective cross-sectional study including patients diagnosed at some point with remitting-relapsing multiple sclerosis (RRMS) or primary progressive multiple sclerosis (PPMS) according to McDonald criteria of 2017 [27] who were systematically followed up in our center's multiple sclerosis. This search includes patients currently labelled as SPMS. This cohort was followed from the time of diagnosis, with visits every 6 months and an annual brain MRI. In addition, supplementary visits and MRIs were conducted as needed in case of relapses.

The inclusion criteria for the study were defined as follows: 1) diagnosis of RRMS or PPMS and systematic follow-up in our MS unit; 2) available MRI scan that includes at least 3DT1TFE and SWI with phase enhancement (SWIp) sequences, both available without intravenous contrast administration, conducted between December 5, 2022 and December 22, 2022. The only exclusion criterion was distortion or limited quality in either of the two imaging sequences.

The European Database for Multiple Sclerosis software was used for a protocolized and validated collection of clinical data [28]. Among the variables collected, the ones used in this study include sex, date of birth, date of symptoms onset, EDSS at the time of MRI, disease subtype at the time of the MRI, disease modifying treatment (DMT) on course at the time of MRI and its initiation date. The following variables were calculated: age at the time of the MRI, age at disease onset, years since disease onset and duration of DMT up to the time of the MRI. The diagnosis criteria for secondary PMS used during follow-up are those previously defined and widely used [29]. DMT were categorized as: "no DMT"; "moderate efficacy DMT" (interferon beta 1a, interferon beta 1b, peginterferon beta 1a, glatiramer acetate, teriflunomide, dimethyl fumarate) and "high efficacy DMT" (fingolimod, natalizumab, alemtuzumab, ocrelizumab, cladribine, or rituximab).

The STROBE guidelines for observational studies were used to conduct this study.

2.3. Imaging

The brain MRIs of the patients who met the inclusion criteria, conducted within the specified date range, were included and analyzed. All MRI examinations were performed using a standardized clinical protocol on the same Achieva 3T scanner (Philips) with a 32-channel head coil. The sequence parameters were identical for all the patients. The specifics of the sequence acquisition parameters are detailed below.

The 3DT1TFE sequence had the following parameters: echo time (TE) was set at 4.9 ms and the repetition time (TR) at 10 ms, with a flip angle of 8°, inversion time 1034 ms; the slice thickness was 1 mm, with in-plane resolution dimensions set at 0.46×0.46 mm^2. The SWIp sequence parameters were as follows: the double TE was set at 7.2 ms and 13.4 ms, the TR was 31 ms, and the flip angle was 17°; the slice thickness was 1.2 mm, with an in-plane resolution of 0.3×0.3 mm^2.

2.4. Image interpretation

The MRI images were jointly reviewed by two neuroradiologists with 5 years and 9 years of sub-specialty experience in MS neuroimaging, respectively [P. N-B. and A. P-E], and discrepancies were resolved by consensus. The data visualization and labeling process was conducted using the RadiAnt DICOM Viewer software (https://www.radiantviewer.com). The images analyzed encompassed three imaging modalities: 3DT1TFE, processed SWIp (from now on only "SWIp"), and SWIp phase. All images for each patient were initially reviewed sequentially in a single session. The review sequence order was randomly assigned in each case. Finally, after the sequential review, any rim lesions identified in any of the three modalities were analyzed and compared simultaneously in the three modalities to retrospectively include lesions that were patent but might have been missed due to human error. This process was carried out to as closely as possible reach the "ground truth" of rim presence.

We identified the T1-dark rim as a peripheral hypointensity surrounding a lesion. The criteria for a T1-dark rim lesion includes a visually appreciable, near-continuous rim of hypointensity bordering the lesion, characterized by its contrast against both the central lesion core and the surrounding brain tissue. Specifically, the contrast window may need to be manually centered by the reader on the hypointense lesion region-range to enhance visualization. We propose to follow similar criteria to identify T1-rims as those proposed for PRLs in a recent

consensus statement for imaging CALs in MS [8], but based on T1-weighted gradient-echo inversion recovery sequences instead of susceptibility-weighted sequences. These criteria would include:

1) A hypointense rim continuous through at least 2/3 of the edge of the WM part of the lesion.
2) The rim corresponds to the edge or at least part of the edge of the T2-hyperintense lesion core.
3) The lesion core is T2-hyperintense and does not enhance on post-contrast weighted imaging.
4) The rim (or part) is discernible on at least 2 consecutive slices (if 2D imaging) or two orthogonal planes (if 3D imaging).

2.5. Lesion classification

SWIp phase imaging was used as the reference standard for "true" PRLs in this study, as prior work has shown that this is more sensitive in terms of visualizing paramagnetic rims than SWIp images [9,30].

Lesions with both a T1-dark rim and a phase rim were considered true positives for a PRL. Lesions with no T1-dark rim but with a phase rim were considered false negatives. Lesions with a T1-dark rim but with no phase rim were categorized as false positives. These false positive lesions were further subclassified based on their appearance on the SWIp images. Specifically, lesions with a T1-dark rim and a hypointense rim on SWIp images were designated "T1-shine-through rims," as we hypothesized that the presence of a rim in these lesions may be justified by a certain T1-shine-through effect [31]. Lesions with a T1-dark rim but with no rim visible on either the SWIp or phase images were designated "isolated T1-dark rims."

2.6. Data analysis

The collected data underwent descriptive and inferential statistical analyses using R software version v4.3.1.

Data are described as mean ± standard deviation (SD) or as median and interquartile range (IQR) according to their distribution. Categorical variables are described using frequencies.

For each imaging volume, the rim lesion frequencies were calculated. For the detection of SWIp phase PRL presence using T1-rim as predictor; sensitivity and positive predictive value (PPV), with exact binomial confidence intervals for each were computed using the "binom" package in R. Furthermore, sensitivity and PPV pairs for rims for each combination of modalities were calculated and presented on a matrix. As the study focused on rim-positive lesions only, the specificity and negative predictive value (NPV) were not considered, as the calculation of these metrics requires the inclusion of true negative cases (i.e., rim-negative lesions), which were not comprehensively included.

3. Results

Overall, 63 patients met the inclusion criteria. The patient selection process is shown in Fig. 1. Detailed demographic and clinical characteristics of the participants, including the sex distribution, age, disease status, disease duration, and disability levels as measured by the EDSS score, are summarized in Table 1.

A total of 80 lesions with a hypointense rim in at least one of the three imaging modalities were detected. Screen captures of all 80 lesions comparing their appearances in the three imaging modalities are presented in the Online Supplemental Data. The highest number of rim lesions was found in 3DT1TFE (78 rims), followed by the SWIp phase (60 rims), and the fewest were found in SWIp (57 rims).

The T1-dark rim, when used to predict the presence of a paramagnetic rim on SWIp phase images, exhibited a sensitivity of 58/60 (96.67 %; exact 95 % confidence interval: 88.47 % to 99.59 %). The positive predictive value was determined to be 58/78 (74.36 %; exact 95 % confidence interval: 63.21 % to 83.58 %). Heatmaps representing the sensitivity and specificity of each combination of imaging modalities included in the study are shown in Fig. 2.

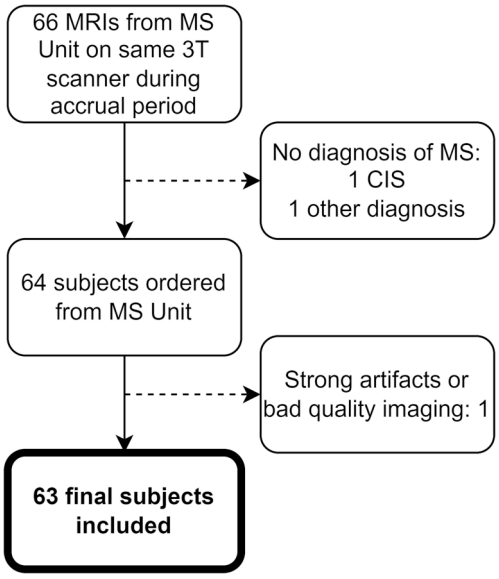

Fig. 1. Patient selection flowchart. Abbreviations: multiple sclerosis (MS), clinically isolated syndrome (CIS).

Table 1
Demographics and clinical characteristics of the study population. Continuous variables are expressed as median values with the interquartile range in parentheses. Categorical variables are shown as patient count integers with the percentage in parenthesis. Abbreviations: Expanded Disability Status Scale (EDSS); relapsing-remitting multiple sclerosis (RRMS); secondary progressive multiple sclerosis (SPMS); primary progressive multiple sclerosis (PPMS), moderate-efficacy disease modifying treatment (ME-DMT), high-efficacy disease modifying treatment (HE-DMT).

Characteristic	Value
Number of subjects	63
Sex (female)	43 (68 %)
Age at MRI [years (IQR)]	49 (43–54.5)
Age at onset [years (IQR)]	30 (23.5–39)
Disease duration [years (IQR)]	14 (6.5–23.5)
Disease status at MRI	
RRMS	52 (83 %)
SPMS	6 (10 %)
PPMS	5 (8 %)
EDSS at MRI (IQR)	2.5 (1.5–5)
Treatment at MRI	
ME-DMT	25 (40 %)
HE-DMT	36 (57 %)
None	2 (3 %)
Years of first-line treatment (IQR)	4.83 (0.17–12.61)
Years of second-line treatment (IQR)	0.48 (0–3.52)

We categorized lesions into true positives, false positives, and false negatives based on their appearance in the 3DT1TFE, SWIp, and SWIp phase imaging. Of the 80 rim lesions identified, 58 were classified as true positives, where both a T1-dark rim and a phase rim were present, regardless of the SWIp-rim appearance. Within the false positive category, 5 lesions were identified as T1-shine-through rims, exhibiting a T1-dark rim and a visible rim on SWIp images but no phase rim. Additionally, 15 lesions were classified as isolated T1-dark rims, marked by the presence of a T1-dark rim but no corresponding rim on either SWIp or phase images. Lastly, 2 lesions were categorized as false negatives, characterized as globally T1-hypointense lesions without a T1-dark rim but with a visible phase rim. Table 2 summarizes the definition and number of lesions identified in each category.

Notably, after further review of the cases of hypointense rims in

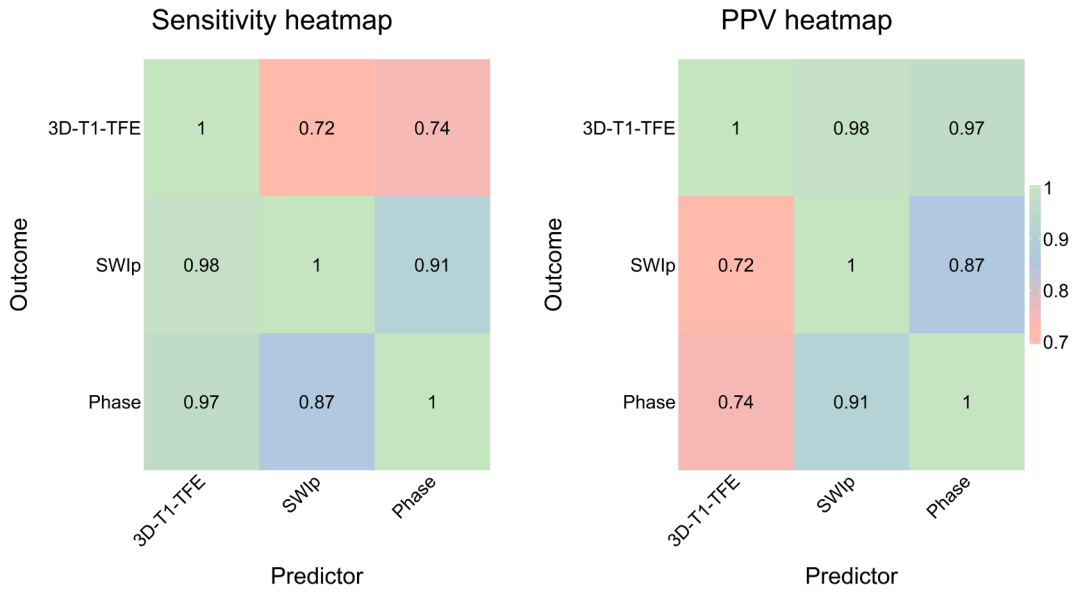

Fig. 2. Sensitivity and positive predictive value (PPV) heatmaps.

Table 2
Summary of the classification of paramagnetic rim lesions based on their appearance in the three imaging modalities, taking the susceptibility-weighted imaging phase as ground truth.

Classification	Definition	Appearance	Number of lesions
True Positive	True paramagnetic rim	T1-rim: Yes Phase-rim: Yes SWIp-rim: Regardless	58
False Positive	T1-shine-through rim	T1-rim: Yes Phase-rim: No SWIp-rim: Yes	5
	Isolated T1-dark rim	T1-rim: Yes Phase-rim: No SWIp-rim: No	15
False Negative	Globally T1-hypointense lesion	T1-rim: No Phase-rim: Yes SWIp-rim: Regardless	2

other modalities that were not present on 3DT1TFE, we identified that in both of these cases, the lesions were globally markedly T1-hypointense in their core. Figs. 3–6 show examples of the four different types of lesions.

4. Discussion

In this study, we have defined the T1-dark rim sign in the MRI exam of patients with MS. This sign, found in 3D T1 gradient-echo inversion-recovery imaging, is highly sensitive and can detect nearly all (97 %) PRLs observed in SWIp phase. However, with a 74 % PPV, over a quarter the of lesions with a T1-dark rim did not have identifiable PRLs on SWIp phase. The clinical significance of these T1-dark rim lesions with no identifiable paramagnetic rim and their possible histopathological relationship with CALs remain unexplored.

The recent shift in MS patient management underscores the importance of accurate prognostic biomarkers. Early high-efficacy disease-modifying treatments can delay disability in patients with high inflammatory activity [3,4]. Additionally, new treatments are effective in non-active progressive MS forms, which previously had no treatment [5,6]. Therefore, markers aiding the early identification of suitable patients are

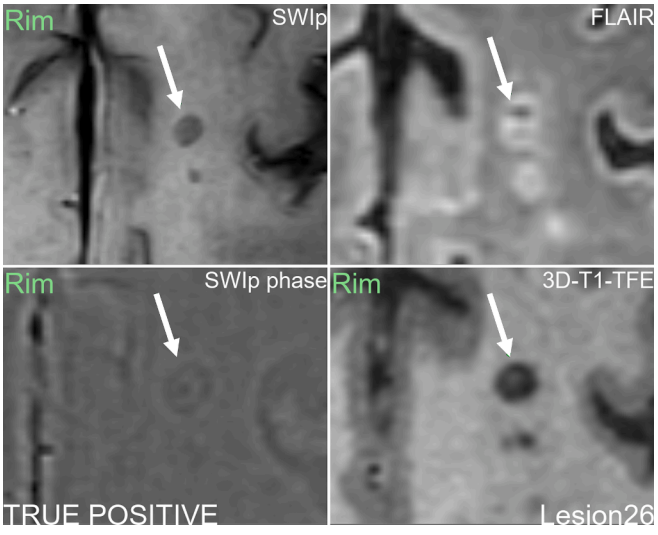

Fig. 3. True positive for paramagnetic rim. The hypointense rim is clearly observed in SWIp phase and 3D-T1-FFE. In this case it can also be seen in SWIp.

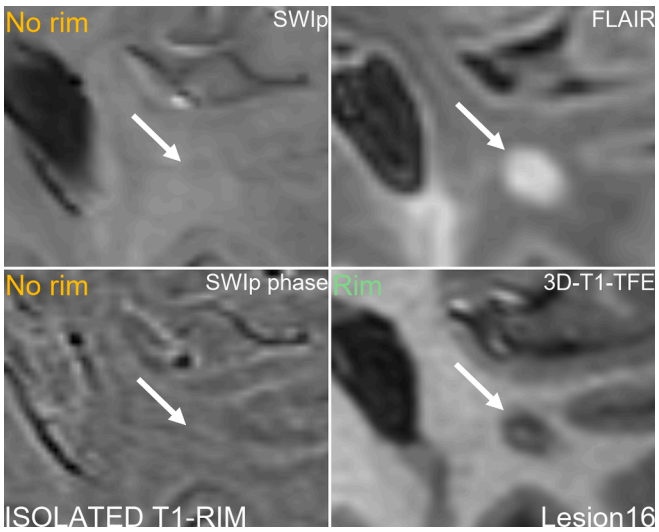

Fig. 4. False positive "isolated T1-dark rim". A T1-dark rim can be observed in 3D-T1TFE, but no rim is present in SWIp or phase.

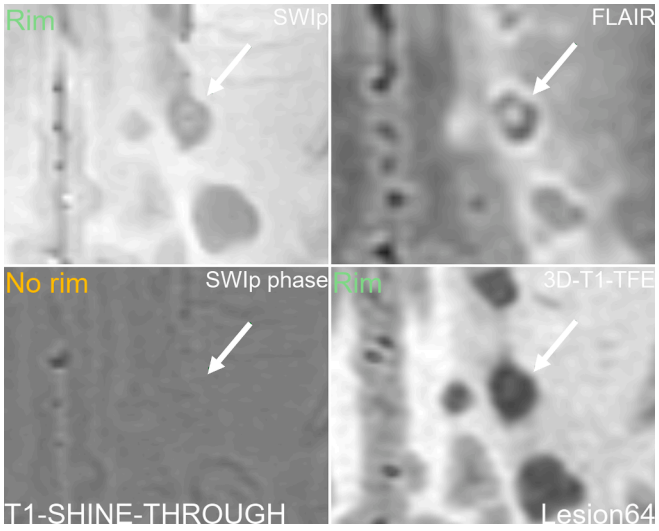

Fig. 5. False positive "T1-shine-through lesion". In the lesion marked by the arrow, there is a T1-rim visible in 3DT1TFE and also in SWIp, but no rim is visible in SWIp phase. Using SWIp phase as ground truth, this corresponds to a false positive. We hypothesize that the SWIp rim might be due to a T1-shine-through effect. Note that apart from the lesion marked with the arrow, two other lesions are visible which do have phase rim.

essential [2].

PRLs, visible in SWI, indicate chronic active inflammation and have been proposed as disability progression biomarkers [15,16]. However, SWI is not routinely used in MS MRI follow-up [17]. Furthermore, these lesions have been primarily characterized using high-field scanners, and lower-field scanners have been less commonly used [12,13,32,33]. Lastly, the identification of PRLs is complex and requires a detailed examination of images, which presents a challenge for their quantification in clinical practice [25].

However, previous studies have described the characteristic T1-hypointensity of PRLs [11,22–24]. Recently, in one study, normalized-intensity 3DT1TFE was used to compare the intensity profiles of PRLs versus non-PRL white-matter lesions, and it was found that a semi-quantifiable deep hypointensity was highly specific to PRLs and, thus, could be studied as a surrogate marker of chronic active inflammation [25]. In the current study, we further built on this concept, and

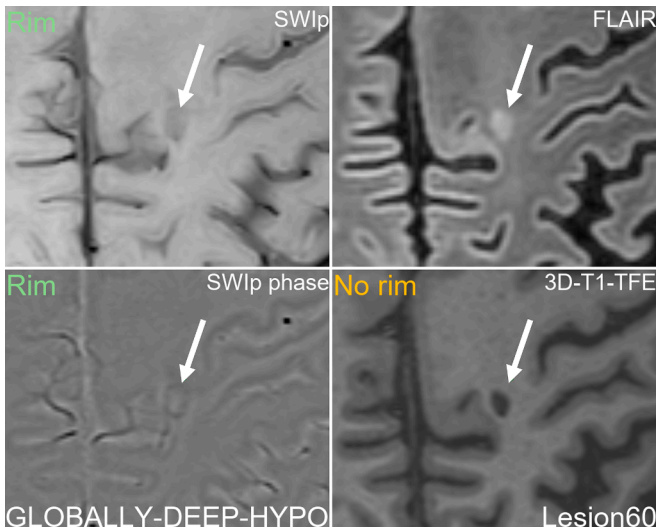

Fig. 6. False negative "globally T1-dark lesion". This lesion has a rim on SWIp and phase, but no rim is visible on 3DT1TFE. However, we can observe that visually the lesion is globally markedly hypointense.

identified that not only are visible T1-hypointense foci present in PRLs, but that they have a characteristic organization as peripheral rims, easily spotted on 3D gradient echo inversion-recovery T1-weighted imaging like 3DT1TFE.

Building on these observations, we postulated that these intensely hypointense voxels might signify active inflammation, unlike "shadow" and "chronic inactive" lesions which are not as hypointense [25]. So, while in acute active lesions, the whole lesion appears hypointense on T1WI [34], our study demonstrates that in CALs, it is the lesion rim that is hypointense, possibly indicating the location of the inflammatory front or active inflammation zone. However, this remains a hypothesis pending further MRI-pathology correlation studies.

While 74 % of T1-dark rim lesions matched with true positive phase-rim lesions, the clinical significance of the remaining 26 % is intriguing. Are they indicative of smoldering inflammation, and do they share the prognostic value of PRLs on SWI? The high sensitivity of T1-dark rims suggests they could be a more sensitive measure for chronic active inflammation than SWI's paramagnetic rims. Contemplating the broader picture of PRLs, it could be suggested that we are witnessing the "tip of the iceberg" regarding chronic active inflammation. For example, slowly-expanding lesions defined on consecutive MRIs are also considered CALs, and they do not always have an accompanying paramagnetic rim on SWI [35,36]. Also, as MRI field strength escalates, PRL detection sensitivity on SWI increases; more lesions surface on 7T than on 3T or 1.5T [12,13,32,33]. This situation leaves us in the dark about the amount of unseen inflammation based on different imaging parameters.

Our research has several inherent strengths, foremost of which is the introduction of the T1-dark rim sign. Indeed, this novel imaging sign serves as a practical alternative to the more advanced SWI techniques for detecting PRLs. Secondly, the image review performed by two neuroradiologists with substantial experience in MS neuroimaging ensured a robust interpretation of the findings. Thirdly, by viewing multiple imaging modalities concurrently in a lesion-centric approach, we ensured a comprehensive and nuanced understanding of the lesion morphologies to enhance the accuracy of our classifications. Finally, the transparent sharing of our imaging data not only solidifies the robustness of our findings but also invites collaboration and scrutiny within the scientific community.

However, the study has limitations. Although we incorporated a second imaging reviewer, we did not execute inter-reviewer correlation. This decision was driven by the aim to be as comprehensive and precise as possible across all sequences, ensuring proximity to the ground truth.

Secondly, SWI is not a standardized sequence, and the characteristics of SWI vary between vendors. This may particularly affect aspects such as the presence of the T1-shine-through effect, which might not necessarily occur when using scanners from other vendors. Lastly, the relatively small size of our subject sample, which was not balanced in terms of disease, prognosis, or demographic characteristics, is another limitation, which prevented us from conducting more comprehensive subject-wise analyses.

5. Conclusions

Our study introduces the T1-dark rim sign as a highly sensitive and accessible imaging marker for the detection of iron-rim lesions. As SWI is not part of standard clinical MS imaging protocols, the T1-dark rim could serve as an alternative marker to identify these lesions, thus potentially enhancing early detection and treatment adjustments for patients with MS at higher risk of disease progression. The findings of this study pave the way for further research to validate the clinical significance and prognostic value of T1-dark rims, which could substantially influence clinical decision-making and patient outcomes in MS.

CRediT authorship contribution statement

Pablo Naval-Baudin: Writing – review & editing, Writing – original draft, Validation, Software, Resources, Project administration, Methodology, Investigation, Formal analysis, Data curation, Conceptualization. **Albert Pons-Escoda:** Writing – review & editing, Writing – original draft, Validation, Methodology, Formal analysis, Data curation, Conceptualization. **Albert Castillo-Pinar:** Writing – review & editing, Writing – original draft, Validation, Methodology, Formal analysis, Data curation, Conceptualization. **Ignacio Martínez-Zalacaín:** Writing – review & editing, Validation, Methodology. **Pablo Arroyo-Pereiro:** Writing – review & editing, Writing – original draft, Validation, Software, Resources, Project administration, Methodology, Investigation, Formal analysis, Data curation, Conceptualization. **Susanie Flores-Casaperalta:** Writing – review & editing, Validation. **Francis Garay-Buitron:** Writing – review & editing, Validation. **Nahum Calvo:** Writing – review & editing, Validation, Supervision, Software, Resources. **Antonio Martinez-Yélamos:** Writing – review & editing, Visualization, Validation, Supervision, Software, Resources, Methodology, Data curation, Conceptualization. **Mónica Cos:** Writing – review & editing, Visualization, Validation, Supervision, Software, Resources, Project administration. **Sergio Martínez-Yélamos:** Writing – review & editing, Visualization, Validation, Supervision, Software, Resources, Data curation, Conceptualization. **Carles Majós:** Writing – review & editing, Writing – original draft, Visualization, Validation, Supervision, Software, Resources, Project administration, Methodology, Investigation, Formal analysis, Data curation, Conceptualization.

Declaration of competing interest

The authors declare that they have no known competing financial interests or personal relationships that could have appeared to influence the work reported in this paper.

Acknowledgements

We extend our gratitude to Ms. Isabel León for her work in extracting clinical data from electronic medical records. Her precise and meticulous efforts have been instrumental to the integrity of our data, thereby contributing significantly to this study.

Appendix A. Supplementary data

Supplementary data to this article can be found online at https://doi.org/10.1016/j.ejrad.2024.111358.

References

[1] D.S. Reich, C.F. Lucchinetti, P.A. Calabresi, Multiple sclerosis, N. Engl. J. Med. 378 (2018) 169–180, https://doi.org/10.1056/NEJMra1401483.

[2] J. Oh, A. Bar-Or, Emerging therapies to target CNS pathophysiology in multiple sclerosis, Nat. Rev. Neurol. 18 (2022) 466–475, https://doi.org/10.1038/s41582-022-00675-0.

[3] K. Harding, O. Williams, M. Willis, J. Hrastelj, A. Rimmer, F. Joseph, V. Tomassini, M. Wardle, T. Pickersgill, N. Robertson, E. Tallantyre, Clinical outcomes of escalation vs early intensive disease-modifying therapy in patients with multiple sclerosis, JAMA Neurol. 76 (2019) 536–541, https://doi.org/10.1001/jamaneurol.2018.4905.

[4] D. Ontaneda, E. Tallantyre, T. Kalincik, S.M. Planchon, N. Evangelou, Early highly effective versus escalation treatment approaches in relapsing multiple sclerosis, Lancet. Neurol. 18 (2019) 973–980, https://doi.org/10.1016/S1474-4422(19)30151-6.

[5] L. Kappos, A. Bar-Or, B.A.C. Cree, R.J. Fox, G. Giovannoni, R. Gold, P. Vermersch, D.L. Arnold, S. Arnould, T. Scherz, C. Wolf, E. Wallström, F. Dahlke, A. Achiron, L. Achtnichts, K. Agan, G. Akman-Demir, A.B. Allen, J.P. Antel, A.R. Antiguedad, M. Apperson, A.M. Applebee, G.I. Ayuso, M. Baba, O. Bajenaru, R. Balasa, B. P. Balci, M. Barnett, A. Bass, V.U. Becker, M. Bejinariu, F.T. Bergh, A. Bergmann, E. Bernitsas, A. Berthele, V. Bhan, F. Bischof, R.J. Bjork, G. Blevins, M. Boehringer, T. Boerner, R. Bonek, J.D. Bowen, A. Bowling, A.N. Boyko, C. Boz, V. Bracknies, S. Braune, V. Brescia Morra, B. Brochet, W. Brola, P.K. Brownstone, M. Brozman, D. Brunet, I. Buraga, M. Burnett, M. Buttmann, H. Butzkueven, J. Cahill, J. C. Calkwood, W. Camu, M. Cascione, G. Castelnovo, D. Centonze, J. Cerqueira, A. Chan, A. Cimprichova, S. Cohan, G. Comi, J. Conway, J.A. Cooper, J. Corboy, J. Correale, B. Costell, D.A. Cottrell, P.K. Coyle, M. Craner, L. Cui, L. Cunha, A. Czlonkowska, A.M. da Silva, J. de Sa, J. de Seze, M. Debouverie, J. Debruyne, D. Decoo, G. Defer, T. Derfuss, N.H. Deri, B. Dihenia, P. Dioszeghy, V. Donath, B. Dubois, M. Duddy, P. Duquette, G. Edan, H. Efendi, S. Elias, P.J. Emrich, B. C. Estruch, E.P. Evdoshenko, J. Faiss, A.S. Fedyanin, W. Feneberg, J. Fermont, O. F. Fernandez, F.C. Ferrer, K. Fink, H. Ford, C. Ford, A. Francia, M. Freedman, B. Frishberg, S. Galgani, G.P. Garmany, K. Gehring, J. Gitt, C. Gobbi, L.P. Goldstick, R.A. Gonzalez, F. Grandmaison, N. Grigoriadis, O. Grigorova, L.M.E. Grimaldi, J. Gross, K. Gross-Paju, M. Gudesblatt, D. Guillaume, J. Haas, V. Hancinova, A. Hancu, O. Hardiman, A. Harmjanz, F.R. Heidenreich, G.J.D. Hengstman, J. Herbert, M. Herring, S. Hodgkinson, O.M. Hoffmann, W.E. Hofmann, W. D. Honeycutt, L.H. Hua, D. Huang, Y. Huang, D. Huang, R. Hupperts, P. Imre, A. K. Jacobs, G. Jakab, E. Jasinska, K. Kaida, J. Kalnina, A. Kaprelyan, G. Karelis, D. Karussis, A. Katz, F.A. Khabirov, B. Khatri, T. Kimura, I. Kister, R. Kizlaitiene, E. Klimova, J. Koehler, A. Komatineni, A. Kornhuber, K. Kovacs, A. Koves, W. Kozubski, G. Krastev, L.B. Krupp, E. Kurca, C. Lassek, G. Laureys, L. Lee, E. Lensch, F. Leutmezer, H. Li, R.A. Linker, M. Linnebank, P. Liskova, C. Llanera, J. Lu, A. Lutterotti, J. Lycke, R. Macdonell, M. Maciejowski, M. Maeurer, R. V. Magzhanov, E.-M. Maida, L. Malciene, Y. Mao-Draayer, G.A. Marfia, C. Markowitz, V. Mastorodimos, K. Matyas, J. Meca-Lallana, J.A.G. Merino, I. G. Mihetiu, I. Milanov, A.E. Miller, A. Millers, M. Mirabella, M. Mizuno, X. Montalban, L. Montoya, M. Mori, S. Mueller, J. Nakahara, Y. Nakatsuji, S. Newsome, R. Nicholas, A.S. Nielsen, E. Nikfekr, U. Nocentini, C. Nohara, K. Nomura, M.M. Odinak, T. Olsson, B.W. van Oosten, C. Oreja-Guevara, P. Oschmann, J. Overell, A. Pachner, G. Panczel, M. Pandolfo, C. Papeix, L. Patrucco, J. Pelletier, R. Piedrabuena, M. Pless, U. Polzer, K. Pozsegovits, D. Rastenyte, S. Rauer, G. Reifschneider, R. Rey, S.A. Rizvi, D. Robertson, J. M. Rodriguez, D. Rog, H. Roshanisefat, V. Rowe, C. Rozsa, S. Rubin, S. Rusek, F. Saccà, T. Saida, A.V. Salgado, V.E.F. Sanchez, K. Sanders, M. Satori, D. V. Sazonov, E.A. Scarpini, E. Schlegel, M. Schluep, S. Schmidt, E. Scholz, H. M. Schrijver, M. Schwab, R. Schwartz, J. Scott, K. Selmaj, S. Shafer, B. Sharrack, I. A. Shchukin, Y. Shimizu, P. Shotekov, A. Siever, K.-O. Sigel, S. Silliman, M. Simo, M. Simu, V. Sinay, A.E. Siquier, A. Siva, O. Skoda, A. Solomon, M. Stangel, D. Stefoski, B. Steingo, I.D. Stolyarov, P. Stourac, K. Strassburger-Krogias, E. Strauss, O. Stuve, I. Tarnev, A. Tavernarakis, C.R. Tello, M. Terzi, V. Ticha, M. Ticmeanu, K. Tiel-Wilck, T. Toomsoo, N. Tubridy, M.J. Tullman, H. Tumani, P. Turcani, B. Turner, A. Uccelli, F.J.O. Urtaza, M. Vachova, A. Valikovics, S. Walter, B. Van Wijmeersch, L. Vanopdenbosch, J.R. Weber, S. Weiss, R. Weissert, P. Vermersch, T. West, H. Wiendl, S. Wiertlewski, B. Wildemann, B. Willekens, L. H. Visser, G. Vorobeychik, X. Xu, T. Yamamura, Y.N. Yang, S.M. Yelamos, M. Yeung, A. Zacharias, M. Zelkowitz, U. Zettl, M. Zhang, H. Zhou, U. Zieman, T. Ziemssen, Siponimod versus placebo in secondary progressive multiple sclerosis (EXPAND): A double-blind, randomised, phase 3 study, Lancet 391 (2018) 1263–1273, https://doi.org/10.1016/S0140-6736(18)30475-6.

[6] J.S. Wolinsky, D.L. Arnold, B. Brochet, H.-P. Hartung, X. Montalban, R.T. Naismith, M. Manfrini, J. Overell, H. Koendgen, A. Sauter, I. Bennett, S. Hubeaux, L. Kappos, S.L. Hauser, Long-term follow-up from the ORATORIO trial of ocrelizumab for primary progressive multiple sclerosis: A post-hoc analysis from the ongoing open-label extension of the randomised, placebo-controlled, phase 3 trial, Lancet Neurol. 19 (2020) 998–1009, https://doi.org/10.1016/S1474-4422(20)30342-2.

[7] E. Tavazzi, R. Zivadinov, M.G. Dwyer, D. Jakimovski, T. Singhal, B. Weinstock-Guttman, N. Bergsland, MRI biomarkers of disease progression and conversion to secondary-progressive multiple sclerosis, Expert Rev. Neurother. 20 (2020) 821–834, https://doi.org/10.1080/14737175.2020.1757435.

[8] F. Bagnato, P. Sati, C.C. Hemond, C. Elliott, S.A. Gauthier, D.M. Harrison, C. Mainero, J. Oh, D. Pitt, R.T. Shinohara, S.A. Smith, B. Trapp, C.J. Azevedo, P.

A. Calabresi, R.G. Henry, C. Laule, D. Ontaneda, W.D. Rooney, N.L. Sicotte, D. S. Reich, M. Absinta, Imaging chronic active lesions in multiple sclerosis: a consensus statement, Brain (2024) 1–18, https://doi.org/10.1093/brain/awae013.
[9] K.E. Hammond, M. Metcalf, L. Carvajal, D.T. Okuda, R. Srinivasan, D. Vigneron, S. J. Nelson, D. Pelletier, Quantitative in vivo magnetic resonance imaging of multiple sclerosis at 7 Tesla with sensitivity to iron, Ann. Neurol. 64 (2008) 707–713, https://doi.org/10.1002/ana.21582.
[10] M. Absinta, P. Sati, M.I. Gaitán, P. Maggi, I.C.M. Cortese, M. Filippi, D.S. Reich, Seven-tesla phase imaging of acute multiple sclerosis lesions: A new window into the inflammatory process, Ann. Neurol. 74 (2013) 669–678, https://doi.org/10.1002/ana.23959.
[11] M. Absinta, P. Sati, M. Schindler, E.C. Leibovitch, J. Ohayon, T. Wu, A. Meani, M. Filippi, S. Jacobson, I.C.M. Cortese, D.S. Reich, Persistent 7-tesla phase rim predicts poor outcome in new multiple sclerosis patient lesions, J. Clin. Invest. 126 (2016) 2597–2609, https://doi.org/10.1172/JCI86198.
[12] F. Bagnato, S. Hametner, B. Yao, P. van Gelderen, H. Merkle, F.K. Cantor, H. Lassmann, J.H. Duyn, Tracking iron in multiple sclerosis: a combined imaging and histopathological study at 7 Tesla, Brain 134 (2011) 3602–3615, https://doi.org/10.1093/brain/awr278.
[13] A. Dal-Bianco, G. Grabner, C. Kronnerwetter, M. Weber, R. Höftberger, T. Berger, E. Auff, F. Leutmezer, S. Trattnig, H. Lassmann, F. Bagnato, S. Hametner, Slow expansion of multiple sclerosis iron rim lesions: pathology and 7 T magnetic resonance imaging, Acta Neuropathol. 133 (2017) 25–42, https://doi.org/10.1007/s00401-016-1636-z.
[14] A. Calvi, C. Tur, D. Chard, J. Stutters, O. Ciccarelli, R. Cortese, M. Battaglini, A. Pietroboni, M. De Riz, D. Galimberti, E. Scarpini, N. De Stefano, F. Prados, F. Barkhof, Slowly expanding lesions relate to persisting black-holes and clinical outcomes in relapse-onset multiple sclerosis, NeuroImage Clin. 35 (2022) 103048, https://doi.org/10.1016/J.NICL.2022.103048.
[15] M. Absinta, P. Sati, F. Masuzzo, G. Nair, V. Sethi, H. Kolb, J. Ohayon, T. Wu, I.C. M. Cortese, D.S. Reich, Association of chronic active multiple sclerosis lesions with disability in vivo, JAMA Neurol. 76 (2019) 1474, https://doi.org/10.1001/jamaneurol.2019.2399.
[16] C.A. Treaba, A. Conti, E.C. Klawiter, V.T. Barletta, E. Herranz, A. Mehndiratta, A. W. Russo, J.A. Sloane, R.P. Kinkel, N. Toschi, C. Mainero, Cortical and phase rim lesions on 7 T MRI as markers of multiple sclerosis disease progression, Brain Commun. 3 (2021) 1–14, https://doi.org/10.1093/braincomms/fcab134.
[17] M.P. Wattjes, O. Ciccarelli, D.S. Reich, B. Banwell, N. de Stefano, C. Enzinger, F. Fazekas, M. Filippi, J. Frederiksen, C. Gasperini, Y. Hacohen, L. Kappos, D.K. B. Li, K. Mankad, X. Montalban, S.D. Newsome, J. Oh, J. Palace, M.A. Rocca, J. Sastre-Garriga, M. Tintoré, A. Traboulsee, H. Vrenken, T. Yousry, F. Barkhof, À. Rovira, M.P. Wattjes, O. Ciccarelli, N. de Stefano, C. Enzinger, F. Fazekas, M. Filippi, J. Frederiksen, C. Gasperini, Y. Hacohen, L. Kappos, K. Mankad, X. Montalban, J. Palace, M.A. Rocca, J. Sastre-Garriga, M. Tintore, H. Vrenken, T. Yousry, F. Barkhof, A. Rovira, D.K.B. Li, A. Traboulsee, S.D. Newsome, B. Banwell, J. Oh, D.S. Reich, D.S. Reich, J. Oh, MAGNIMS–CMSC–NAIMS consensus recommendations on the use of MRI in patients with multiple sclerosis, Lancet Neurol. 20 (2021) (2021) 653–670, https://doi.org/10.1016/S1474-4422(21)00095-8.
[18] J.-C. Brisset, S. Kremer, S. Hannoun, F. Bonneville, F. Durand-Dubief, T. Tourdias, C. Barillot, C. Guttmann, S. Vukusic, V. Dousset, F. Cotton, R. Ameli, R. Anxionnat, B. Audoin, A. Attye, E. Bannier, C. Barillot, D. Ben Salem, M.-P. Boncoeur-Martel, G. Bonhomme, F. Bonneville, C. Boutet, J.C. Brisset, F. Cervenanski, B. Claise, O. Commowick, J.-M. Constans, F. Cotton, P. Dardel, H. Desal, V. Dousset, F. Durand-Dubief, J.-C. Ferre, A. Gaultier, E. Gerardin, T. Glattard, S. Grand, T. Grenier, R. Guillevin, C. Guttmann, A. Krainik, S. Kremer, S. Lion, N.M. De Champfleur, L. Mondot, O. Outteryck, N. Pyatigorskaya, J.-P. Pruvo, S. Rabaste, J.-P. Ranjeva, J.-A. Roch, J.-C. Sadik, D. Sappey-Marinier, J. Savatovsky, B. Stankoff, J.-Y. Tanguy, A. Tourbah, T. Tourdias, B. Brochet, R. Casey, F. Cotton, J. De Sèze, P. Douek, F. Guillemin, D. Laplaud, C. Lebrun-Frenay, L. Mansuy, T. Moreau, J. Olaiz, J. Pelletier, C. Rigaud-Bully, B. Stankoff, S. Vukusic, M. Debouverie, G. Edan, J. Ciron, C. Lubetzki, P. Vermersch, P. Labauge, G. Defer, E. Berger, P. Clavelou, O. Gout, E. Thouvenot, O. Heinzlef, A. Al-Khedr, B. Bourre, O. Casez, P. Cabre, A. Montcuquet, A. Créange, J.-P. Camdessanché, S. Bakchine, A. Maurousset, I. Patry, T. De Broucker, C. Pottier, J.-P. Neau, C. Labeyrie, C. Nifle, New OFSEP recommendations for MRI assessment of multiple sclerosis patients: Special consideration for gadolinium deposition and frequent acquisitions, J. Neuroradiol. 47 (2020) 250–258, https://doi.org/10.1016/j.neurad.2020.01.083.
[19] G. Barquero, F. La Rosa, H. Kebiri, P.-J. Lu, R. Rahmanzadeh, M. Weigel, M. J. Fartaria, T. Kober, M. Théaudin, R. Du Pasquier, P. Sati, D.S. Reich, M. Absinta, C. Granziera, P. Maggi, M. Bach Cuadra, RimNet: A deep 3D multimodal MRI architecture for paramagnetic rim lesion assessment in multiple sclerosis, NeuroImage Clin. 28 (2020) 102412, https://doi.org/10.1016/j.nicl.2020.102412.
[20] C. Lou, P. Sati, M. Absinta, K. Clark, J.D. Dworkin, A.M. Valcarcel, M.K. Schindler, D.S. Reich, E.M. Sweeney, R.T. Shinohara, Fully automated detection of paramagnetic rims in multiple sclerosis lesions on 3T susceptibility-based MR imaging, NeuroImage Clin. 32 (2021) 102796, https://doi.org/10.1016/j.nicl.2021.102796.
[21] H. Zhang, T.D. Nguyen, J. Zhang, M. Marcille, P. Spincemaille, Y. Wang, S. A. Gauthier, E.M. Sweeney, QSMRim-Net: Imbalance-aware learning for identification of chronic active multiple sclerosis lesions on quantitative susceptibility maps, NeuroImage Clin. 34 (2022) 102979, https://doi.org/10.1016/j.nicl.2022.102979.
[22] C. Elliott, S. Belachew, J.S. Wolinsky, S.L. Hauser, L. Kappos, F. Barkhof, C. Bernasconi, J. Fecker, F. Model, W. Wei, D.L. Arnold, Chronic white matter lesion activity predicts clinical progression in primary progressive multiple sclerosis, Brain 142 (2019) 2787–2799, https://doi.org/10.1093/brain/awz212.
[23] A. Calvi, L. Haider, F. Prados, C. Tur, D. Chard, F. Barkhof, In vivo imaging of chronic active lesions in multiple sclerosis, Mult. Scler. J. 28 (2022) 683–690, https://doi.org/10.1177/1352458520958589.
[24] K.C. Ng Kee Kwong, D. Mollison, R. Meijboom, E.N. York, A. Kampaite, S.-J. Martin, D.P.J. Hunt, M.J. Thrippleton, S. Chandran, A.D. Waldman, FutureMS consortium, Rim lesions are demonstrated in early relapsing-remitting multiple sclerosis using 3 T-based susceptibility-weighted imaging in a multi-institutional setting, Neuroradiology 64 (2022) 109–117, https://doi.org/10.1007/s00234-021-02768-x.
[25] P. Naval-Baudin, A. Pons-Escoda, À. Camins, P. Arroyo, M. Viveros, J. Castell, M. Cos, A. Martínez-Yélamos, S. Martínez-Yélamos, C. Majós, Deeply 3D–T1-TFE hypointense voxels are characteristic of phase-rim lesions in multiple sclerosis, Eur. Radiol. Online Ahe (2023), https://doi.org/10.1007/s00330-023-09784-w.
[26] S. Choi, S. Lake, D.M. Harrison, Evaluation of the blood-brain barrier, demyelination, and neurodegeneration in paramagnetic rim lesions in multiple sclerosis on 7 tesla <scp>MRI</scp>, J. Magn. Reson. Imaging (2023), https://doi.org/10.1002/jmri.28847.
[27] A.J. Thompson, B.L. Banwell, F. Barkhof, W.M. Carroll, T. Coetzee, G. Comi, J. Correale, F. Fazekas, M. Filippi, M.S. Freedman, K. Fujihara, S.L. Galetta, H. P. Hartung, L. Kappos, F.D. Lublin, R.A. Marrie, A.E. Miller, D.H. Miller, X. Montalban, E.M. Mowry, P.S. Sorensen, M. Tintoré, A.L. Traboulsee, M. Trojano, B.M.J. Uitdehaag, S. Vukusic, E. Waubant, B.G. Weinshenker, S.C. Reingold, J. A. Cohen, Diagnosis of multiple sclerosis: 2017 revisions of the McDonald criteria, Lancet Neurol. 17 (2018) 162–173, https://doi.org/10.1016/S1474-4422(17)30470-2.
[28] C. Confavreux, D.A. Compston, O.R. Hommes, W.I. McDonald, A.J. Thompson, EDMUS, a European database for multiple sclerosis, J. Neurol. Neurosurg. Psychiatry 55 (1992) 671–676, https://doi.org/10.1136/jnnp.55.8.671.
[29] J. Lorscheider, K. Buzzard, V. Jokubaitis, T. Spelman, E. Havrdova, D. Horakova, M. Trojano, G. Izquierdo, M. Girard, P. Duquette, A. Prat, A. Lugaresi, F. Grand'Maison, P. Grammond, R. Hupperts, R. Alroughani, P. Sola, C. Boz, E. Pucci, J. Lechner-Scott, R. Bergamaschi, C. Oreja-Guevara, G. Iuliano, V. Van Pesch, F. Granella, C. Ramo-Tello, D. Spitaleri, T. Petersen, M. Slee, F. Verheul, R. Ampapa, M.P. Amato, P. McCombe, S. Vucic, J.L. Sánchez Menoyo, E. Cristiano, M.H. Barnett, S. Hodgkinson, J. Olascoaga, M.L. Saladino, O. Gray, C. Shaw, F. Moore, H. Butzkueven, T. Kalincik, MSBase study group, defining secondary progressive multiple sclerosis, Brain 139 (2016) 2395–2405, https://doi.org/10.1093/brain/aww173.
[30] M.S. Martire, L. Moiola, M.A. Rocca, M. Filippi, M. Absinta, What is the potential of paramagnetic rim lesions as diagnostic indicators in multiple sclerosis? Expert Rev. Neurother. 22 (2022) 829–837, https://doi.org/10.1080/14737175.2022.2143265.
[31] C.-C.-T. Hsu, E.M. Haacke, C.C. Heyn, T.W. Watkins, T. Krings, The T1 shine through effect on susceptibility weighted imaging: an under recognized phenomenon, Neuroradiology 60 (2018) 235–237, https://doi.org/10.1007/s00234-018-1977-5.
[32] C.C. Hemond, D.S. Reich, S.K. Dundamadappa, Paramagnetic rim lesions in multiple sclerosis: Comparison of visualization at 1.5-T and 3-T MRI, Am. J. Roentgenol. 219 (2022) 120–131, https://doi.org/10.2214/AJR.21.26777.
[33] K.C. Ng Kee Kwong, D. Mollison, R. Meijboom, E.N. York, A. Kampaite, M. J. Thrippleton, S. Chandran, A.D. Waldman, The prevalence of paramagnetic rim lesions in multiple sclerosis: A systematic review and meta-analysis, PLoS One 16 (2021) e0256845, https://doi.org/10.1371/journal.pone.0256845.
[34] À. Rovira, C. Auger, J. Alonso, Magnetic resonance monitoring of lesion evolution in multiple sclerosis, Ther. Adv. Neurol. Disord. 6 (2013) 298–310, https://doi.org/10.1177/1756285613484079.
[35] A. Calvi, M.A. Clarke, F. Prados, D. Chard, O. Ciccarelli, M. Alberich, D. Pareto, M. Rodríguez Barranco, J. Sastre-Garriga, C. Tur, A. Rovira, F. Barkhof, Relationship between paramagnetic rim lesions and slowly expanding lesions in multiple sclerosis, Mult. Scler. 29 (2023) 352–362, https://doi.org/10.1177/13524585221141964.
[36] C. Elliott, D.A. Rudko, D.L. Arnold, D. Fetco, A.M. Elkady, D. Araujo, B. Zhu, A. Gafson, Z. Tian, S. Belachew, D.P. Bradley, E. Fisher, Lesion-level correspondence and longitudinal properties of paramagnetic rim and slowly expanding lesions in multiple sclerosis, Mult. Scler. 29 (2023) 680–690, https://doi.org/10.1177/13524585231162262.